

Products of the Gas-Phase Reaction of the OH Radical with 3-Methyl-1-Butene in the Presence of NO

ROGER ATKINSON,* ERNESTO C. TUAZON, SARA M. ASCHMANN

Air Pollution Research Center, University of California, Riverside, California 92521

Received 29 September 1997; accepted 26 February 1998

ABSTRACT: The products of the gas-phase reaction of the OH radical with 3-methyl-1-butene in the presence of NO have been investigated at room temperature and 740 torr total pressure of air by gas chromatography with flame ionization detection, in situ Fourier transform infrared absorption spectroscopy, and direct air sampling atmospheric pressure ionization tandem mass spectrometry. The products identified and quantified by GC-FID and in situ FT-IR absorption spectroscopy were HCHO, 2-methylpropanal, acetone, glycolaldehyde, and methacrolein, with formation yields of 0.70 ± 0.06 , 0.58 ± 0.08 , 0.17 ± 0.02 , 0.18 ± 0.03 , and 0.033 ± 0.007 , respectively. In addition, IR absorption bands due to organic nitrates were observed, consistent with API-MS observations of product ion peaks attributed to the β -hydroxynitrates $(\text{CH}_3)_2\text{CHCH}(\text{ONO}_2)\text{CH}_2\text{OH}$ and/or $(\text{CH}_3)_2\text{CHCH}(\text{OH})\text{CH}_2\text{ONO}_2$ formed from the reactions of the corresponding β -hydroxyalkyl peroxy radicals with NO. A formation yield of ca. 0.15 for these nitrates was estimated using IR absorption band intensities for known organic nitrates. These products account for essentially all of the reacted 3-methyl-1-butene. Analysis of the potential reaction pathways involved shows that H-atom abstraction from the allylic C—H bond in 3-methyl-1-butene is a minor pathway which accounts for 5–10% of the overall OH radical reaction. © 1998 John Wiley & Sons, Inc. *Int J Chem Kinet*: 30: 577–587, 1998

INTRODUCTION

Alkenes are a significant component of ambient air in urban areas [1–3] and react with OH radicals, NO_3 radicals, and O_3 in the troposphere [4,5], with the day-

time OH radical reaction often dominating as the alkene removal process [6,7]. While the kinetics of the gas-phase reactions of the OH radical with alkenes have been studied previously [4,5,8] and are reasonably reliably known [5], few product studies have been conducted at atmospheric pressure of air for simple acyclic alkenes [5,9–18]. Kinetic and product data show that at room temperature and atmospheric pressure the OH radical reactions proceed mainly by addition to the $> \text{C}=\text{C} <$ bond [4,5,8]. Extrapolations of rate constants measured at elevated temperatures ($> 600 \text{ K}$) [4,8] indicate that the fractions of the OH radical reactions with ethene, propene, and 1-butene which proceed by H-atom abstraction at 298 K are ca.

* Also, Environmental Toxicology Graduate Program and the Departments of Environmental Science and Chemistry, University of California, Riverside, California 92521

Correspondence to: R. Atkinson

Contract grant Sponsor: U.S. Environmental Protection Agency, Office of Research and Development

Contract grant number: Assistance Agreement R-825252-01-0

Contract grant Sponsor: National Science Foundation

Contract grant number: Grant No. ATM-9015361

Contract grant Sponsor: University of California, Riverside

© 1998 John Wiley & Sons, Inc. CCC 0538-8066/98/080577-11

0.1%, ca. 3%, and ca. 7%, respectively [4,8]. Rate constants measured at 1237–1275 K for 2-methylpropene, *trans*-2-butene, and 2,3-dimethyl-2-butene [19] are also consistent with H-atom abstraction accounting for ca. 2–3% of the overall OH radical reaction at 298 K [8]. Product studies of the reactions of the OH radical with propene, 1-butene, 2-methylpropene, *cis*-2-butene, and *trans*-2-butene [11,20,21] have concluded that H-atom abstraction is minor at room temperature and atmospheric pressure (<5%, <10%, <5%, <10%, and <10%, respectively).

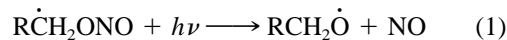
The bond dissociation energies of the allylic C—H bonds in propene, 1-butene, and 3-methyl-1-butene are 86.3 ± 1.5 , 82.5 ± 1.3 , and 77.2 ± 1.5 kcal mol⁻¹, respectively [22,23]. Extrapolation of the estimated H-atom abstraction rate constants for propene and 1-butene [4,8] to 3-methyl-1-butene, assuming a linear correlation of ln (H-atom abstraction rate constant at 298 K) against the allylic C—H bond dissociation energy, suggests that H-atom abstraction from the allylic C—H bond in 3-methyl-1-butene could account for ca. 30% of the overall reaction at 298 K and atmospheric pressure. We have used gas chromatography with flame ionization detection (GC-FID), in situ atmospheric pressure ionization tandem mass spectrometry (API-MS), and in situ Fourier transform infrared absorption spectroscopy (FT-IR) to investigate the products formed from the gas-phase reaction of the OH radical with 3-methyl-1-butene at room temperature and atmospheric pressure of air.

EXPERIMENTAL

Experiments were carried out in a 5800 liter evacuable, Teflon-coated chamber containing an in situ multiple reflection optical system interfaced to a Nicolet 7199 FT-IR absorption spectrometer and with irradiation provided by a 24-kW xenon arc filtered through a 0.25 in. thick Pyrex pane (to remove wavelengths <300 nm), in a 7900 liter Teflon chamber with analysis by GC-FID and with irradiation provided by two parallel banks of blacklamps, and in a second 7900 liter Teflon chamber interfaced to a PE SCIEX API III MS/MS direct air sampling, atmospheric pressure ionization tandem mass spectrometer (API-MS), again with irradiation provided by two parallel banks of blacklamps. All three chambers are fitted with Teflon-coated fans to ensure rapid mixing of reactants during their introduction into the chamber.

Hydroxyl radicals were generated by the photolysis of methyl nitrite (CH₃ONO) or ethyl nitrite

(C₂H₅ONO) in air at wavelengths >300 nm [11,12,24]:



where R = H or CH₃. NO was added to the reactant mixtures to suppress the formation of O₃ and, hence, of NO₃ radicals [24]. Because HCHO is the primary photolytic product of methyl nitrite (see above) and HCHO is expected to be a major product of the OH radical-initiated reaction of 3-methyl-1-butene in the presence of NO [5], the photolysis of ethyl nitrite in air was used as the OH radical source for the determination of HCHO formation yields in the 5800 liter evacuable chamber. In the 7900 liter Teflon chambers with analyses by GC-FID and API-MS, OH radicals were generated by the photolysis of CH₃ONO in air.

Teflon Chamber with Analysis by GC-FID

The initial reactant concentrations (in molecule cm⁻³ units) were: CH₃ONO, ca. 2.4×10^{14} ; NO, ca. 2.4×10^{14} ; and 3-methyl-1-butene, $(2.03\text{--}2.29) \times 10^{13}$. Irradiations were carried out at 20% of the maximum light intensity for 4–12 mins, resulting in reaction of up to 62% of the initially present 3-methyl-1-butene. The concentrations of 3-methyl-1-butene were measured during the experiments by GC-FID as described previously [25]. The concentrations of certain carbonyl products were measured by GC-FID by collecting 100 cm³ volume gas samples from the chamber onto Tenax-TA solid adsorbent, with subsequent thermal desorption at ca. 225°C onto a 30 m DB-1701 megabore column in a Hewlett Packard (HP) 5710 GC, initially held at -40°C and then temperature programmed at 8°C min⁻¹ to 200°C. GC-FID response factors were measured as described previously [25,26]. In addition, combined gas chromatography-mass spectrometry (GC-MS) analyses of samples collected on Tenax solid adsorbent were carried out using a 30 m DB-1701 fused silica capillary column in a HP 5890 GC interfaced to a HP 5971 Mass Selective Detector, operating in the scanning mode.

Evacuatable Chamber with Analysis by FT-IR Absorption Spectroscopy

The initial concentrations of 3-methyl-1-butene, ethyl nitrite, and NO in the two experiments carried out were 4.92×10^{14} molecule cm⁻³, 2.46×10^{14} mole-

cule cm^{-3} , and $(1.85\text{--}3.08) \times 10^{14}$ molecule cm^{-3} , respectively. In the first experiment which employed an initial NO concentration of 1.85×10^{14} molecule cm^{-3} , an additional 1.85×10^{14} molecule cm^{-3} of NO was added halfway through the experiment. Partial pressures of 3-methyl-1-butene, ethyl nitrite, and NO were measured into calibrated 5 liter and 2 liter Pyrex bulbs with an MKS Baratron 0–100 torr sensor and flushed into the 5800 liter chamber with N_2 gas. Four intermittent irradiations of 1.0–3.0 min duration were carried out during each experiment, resulting in reaction of up to 25% of the initially present 3-methyl-1-butene. Analyses by FT-IR spectroscopy were carried out during the dark periods, with 64 coadded interferograms (scans) per spectrum (1.8 min measurement time) being recorded with a full width at half-maximum (fwhm) resolution of 0.7 cm^{-1} and a pathlength of 62.9 m. The product spectra were analyzed by desynthesis, which consisted of successively subtracting the absorptions of known compounds with the use of calibrated reference spectra. The methods employed in the calibration and subtractive analysis have been described in detail previously [27]. IR reference spectra of the products measured were available from previous calibrations in this laboratory [27].

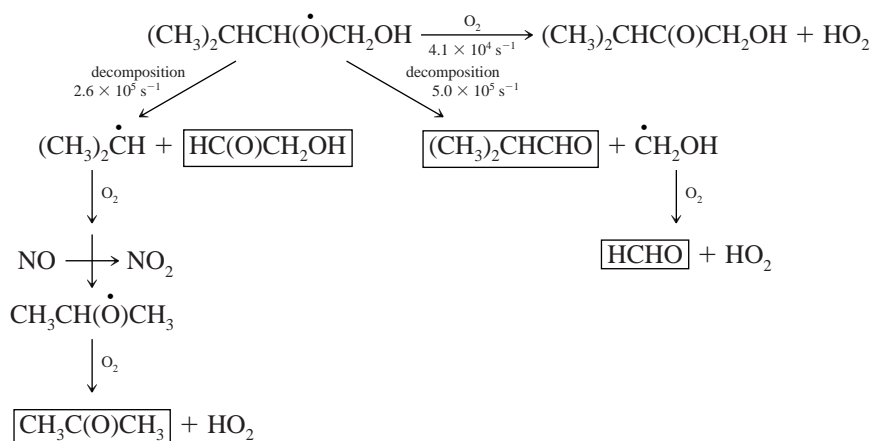
Teflon Chamber with Analysis by API-MS

The PE SCIEX API III MS/MS instrument was interfaced to the Teflon chamber via a 25 mm diameter \times 75 cm length Pyrex tube, and the chamber contents were sampled at a flow rate of ca. 20 liter min^{-1} directly into the API mass spectrometer source. The operation of the API-MS in the MS (scanning) and MS/MS [with collision activated dissociation (CAD)] modes has been described elsewhere [17,18,28,29].

The MS/MS mode allows the “daughter ion” or “parent ion” spectrum of a given ion peak observed in the MS scanning mode to be obtained [17,18,28,29]. The positive ion mode was used in this work, with protonated water hydrates ($\text{H}_3\text{O}^+(\text{H}_2\text{O})_n$) generated by the corona discharge in the chamber diluent gas being responsible for the protonation of analytes. Ions are drawn by an electric potential from the ion source through the sampling orifice into the mass-analyzing first quadrupole or third quadrupole. For these experiments, the API-MS instrument was operated under conditions that favored the formation of dimer ions in the ion source region [28–30]. Neutral molecules and particles are prevented from entering the orifice by a flow of high-purity nitrogen (“curtain” gas), and as a result of the declustering action of the curtain gas on the hydrated ions, the ions that are mass-analyzed are mainly protonated molecular ions ($[\text{M} + \text{H}]^+$) and their protonated homo- and hetero-dimers [17,18,28–30]. The initial concentrations of CH_3ONO , NO, and 3-methyl-1-butene were ca. 4.8×10^{13} molecule cm^{-3} each, and irradiations were carried out for 3 min at 20% of the maximum light intensity.

Chemicals

The chemicals used, and their stated purities, were: acetone, >99.6% (Fisher Scientific); methacrolein (95%), 3-methyl-2-butenal (97%), 2-methylpropanal (99 + %), and methyl vinyl ketone (99%), Aldrich Chemical Company; NO ($\geq 99.0\%$), Matheson Gas Products; and 3-methyl-1-butene (99 + %), Liquid Carbonic. Methyl nitrite was prepared as described by Taylor *et al.* [31] and was stored at 77 K under vacuum.

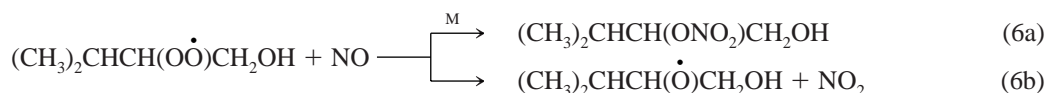


Reaction Scheme I

RESULTS

Reaction Schemes I and II show the reaction mechanisms and the products which can be formed from the alkoxy radicals $(\text{CH}_3)_2\text{CHCH}(\dot{\text{O}})\text{CH}_2\text{OH}$ and

$(\text{CH}_3)_2\text{CHCH}(\text{OH})\text{CH}_2\dot{\text{O}}$, produced after initial OH radical addition to the 1- and 2-positions through the reactions illustrated for OH radical addition at the 1-position [5],

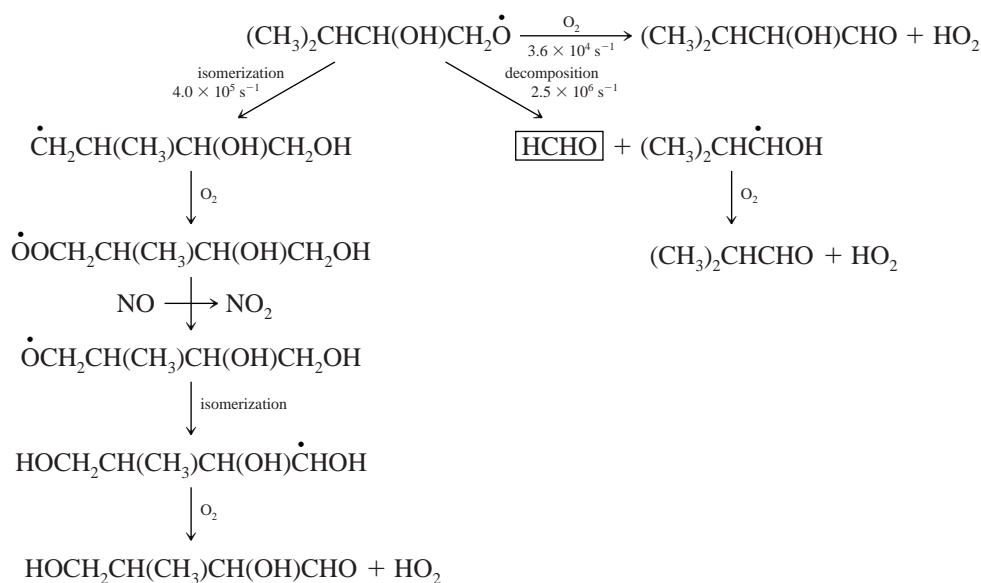


and similarly for OH radical addition at the 2-position. Reaction Scheme III shows the reaction mechanisms and the products which can be formed from the $(\text{CH}_3)_2\dot{\text{C}}\text{HCH}=\text{CH}_2$ radical formed after H-atom abstraction from the allylic C—H bond of the carbon atom at the 3-position. For clarity, organic nitrate formation from the reactions of RO_2 radicals with NO [5] via Reaction (6a) and analogous reactions is omitted from Reaction Schemes I–III. Also, shown in Reaction Schemes I–III are the estimated reaction rates of the important alkoxy radicals involved, calculated as described by Atkinson [32]. H-atom abstraction from the two $-\text{CH}_3$ groups in 3-methyl-1-butene is estimated to account for only ca. 1% of the overall OH radical reaction [33], and the subsequent reactions of the $\dot{\text{C}}\text{H}_2\text{CH}(\text{CH}_3)\text{CH}=\text{CH}_2$ radical are expected [5,32] to lead to the formation of methyl vinyl ketone plus formaldehyde. The potential products shown in Reaction Schemes I through III form the basis for

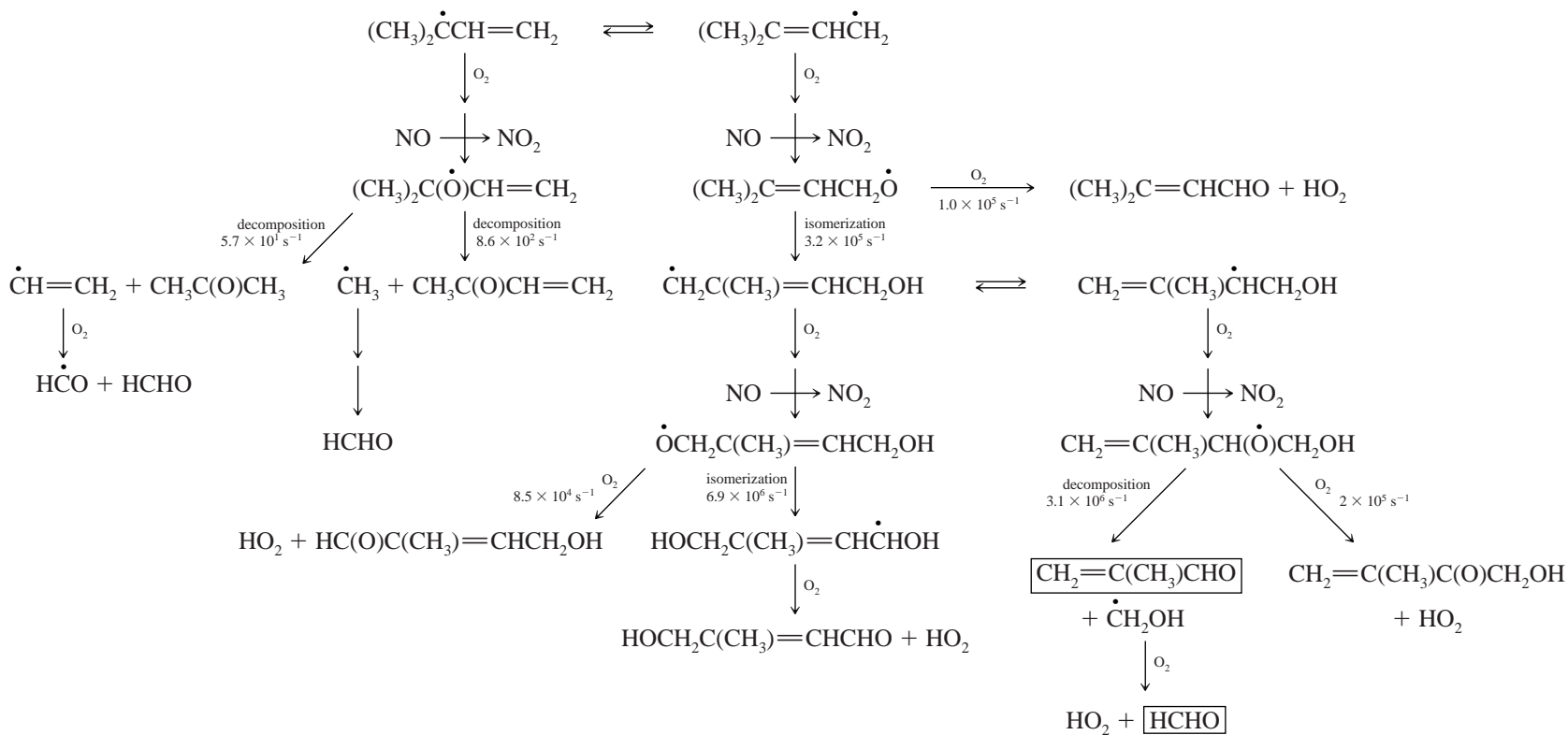
the discussion (observed products are shown by “boxes”).

Teflon Chamber with GC-FID Analyses and Evacuatable Chamber with FT-IR Analyses

GC-FID and GC-MS analyses of irradiated $\text{CH}_3\text{-ONO-NO-3-methyl-1-butene-air}$ mixtures showed the formation of acetone, 2-methylpropanal, and methacrolein [$\text{CH}_2=\text{C}(\text{CH}_3)\text{CHO}$]. However, no evidence was obtained from the GC-FID and GC-MS analyses for the formation of methyl vinyl ketone [$\text{CH}_3\text{C}(\text{O})\text{CH}=\text{CH}_2$] or 3-methyl-2-butenal [$(\text{CH}_3)_2\text{C}=\text{CHCHO}$], and upper limits to the amounts of these two products were obtained from conservative limits of detection of the GC-FID analyses. FT-IR analyses of irradiated $\text{C}_2\text{H}_5\text{ONO-NO-3-methyl-1-butene-air}$ mixtures showed the formation of 2-methylpropanal, HCHO, acetone, glycolaldehyde



Reaction Scheme II



Reaction Scheme III

[HOCH₂CHO], methacrolein, and unidentified organic nitrates.

The results of FT-IR analyses for the two irradiations conducted in the 5800 liter chamber were similar, except for the formation of small amounts of HOONO₂ in the first experiment after NO was consumed, which was suppressed as a second aliquot of NO was added. NO remained in excess throughout the second experiment, which employed a higher initial NO concentration. Product spectra from the latter experiment, after a cumulative irradiation time of 9 min, are shown in Figure 1. Figure 1(A) is the spectrum of the products which are attributable to 3-methyl-1-butene, obtained after subtraction of absorptions by the remaining reactants and products associated with irradiated C₂H₅ONO-NO-air mixtures [CH₃CHO, C₂H₅ONO₂, CH₃C(O)OONO₂ (PAN), NO₂, HNO₃, HONO, and HC(O)OH]. The subtractive steps depicted in Figure 1(A)–(C) reveal the components of the overlapping absorptions in the 1740 cm⁻¹ region. In Figure 1(C), prominent absorption bands at 852, 1284, and 1658 cm⁻¹ indicate the presence of an organic nitrate(s), RONO₂. A distinct absorption band at 1035 cm⁻¹, most likely due to a C—O stretch, is consistent with the API-MS results

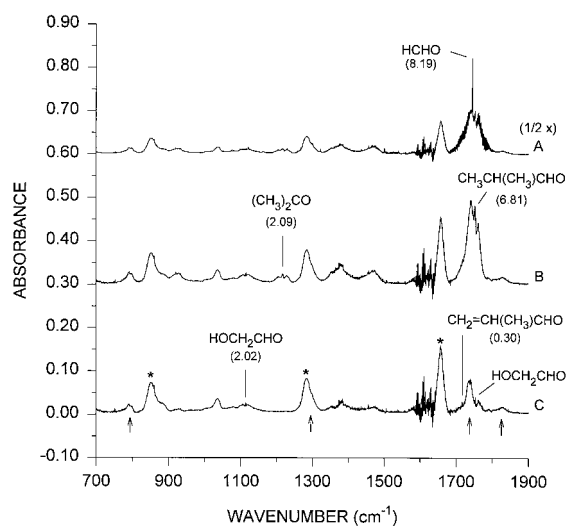


Figure 1 Infrared spectra from a C₂H₅ONO-NO-3-methyl-1-butene-air irradiation. (A) Products attributed to reaction of 3-methyl-1-butene (see text) after 9 min of photolysis, with 1.24×10^{14} molecule cm⁻³ of 3-methyl-1-butene consumed. (B) From (A) after subtraction of HCHO absorptions. (C) From (B) after subtraction of absorptions due to acetone and 2-methylpropanal. Asterisks denote RONO₂-type absorption bands, while arrows indicate RC(O)OONO₂-type absorption bands. The numbers in parentheses are concentrations in units of 10¹³ molecule cm⁻³.

(see below) that the RONO₂ compounds formed contain hydroxyl groups (the weak O—H stretch absorption band near 3700 cm⁻¹ was beyond the optimal range of the IR detector). The formation of a peroxyacyl nitrate, most likely (CH₃)₂CHC(O)OONO₂, which became more important during the latter part of the irradiation, is indicated by the characteristic “PAN-type” absorption bands at 794, 1300, 1738, and 1830 cm⁻¹.

The observed products also react with the OH radical [4,8] and, hence, their secondary reactions must be considered in deriving their formation yields (or upper limits thereof). Secondary reactions of the observed or (for methyl vinyl ketone and 3-methyl-2-butenal) potential products with the OH radical were taken into account as described previously [34], using the recommended OH radical reaction rate constants for 3-methyl-1-butene, acetone, 2-methylpropanal, HCHO, glycolaldehyde, methacrolein, and methyl vinyl ketone [4,5,8] and the estimated rate constant for 3-methyl-2-butenal [33]. The multiplicative correction factors to the measured product concentrations to take into account these secondary reactions depend on the rate constant ratio $k(\text{OH}) + \text{product}/k(\text{OH} + 3\text{-methyl-1-butene})$ and increase with increasing extent of reaction and were therefore larger for the experiments in the Teflon chamber with GC-FID analyses than in the evacuable chamber with FT-IR analyses. The maximum calculated values of the multiplicative factors were: for 2-methylpropanal, 1.55 (experiments with GC-FID analyses) and 1.13 (experiments with FT-IR analyses); acetone, < 1.004 in all cases; methacrolein, 1.73 (experiments with GC-FID analyses) and 1.17 (experiments with FT-IR analyses); methyl vinyl ketone, 1.35; 3-methyl-2-butenal, 2.02; HCHO, 1.05; and glycolaldehyde, 1.05. The reaction of the OH radical with 2-methylpropanal may be expected to lead to the formation of acetone and/or the peroxyacyl nitrate (CH₃)₂CHC(O)OONO₂, depending on the NO/NO₂ concentration ratio [4]. Additionally, the formation of small amounts of HCHO from the reaction of the OH radical with acetaldehyde (the major product from the photolysis of ethyl nitrite) is also expected [16] in the experiments carried out in the evacuable chamber with FT-IR analyses. These possibilities of secondary formation of acetone and HCHO are discussed below.

Figure 2 shows plots of the amounts of HCHO, 2-methylpropanal, acetone, glycolaldehyde, and methacrolein formed, corrected for reaction with the OH radical, against the amounts of 3-methyl-1-butene reacted in the evacuable chamber experiments with FT-IR analyses, while Figure 3 shows analogous plots for the formation of 2-methylpropanal, acetone, and meth-

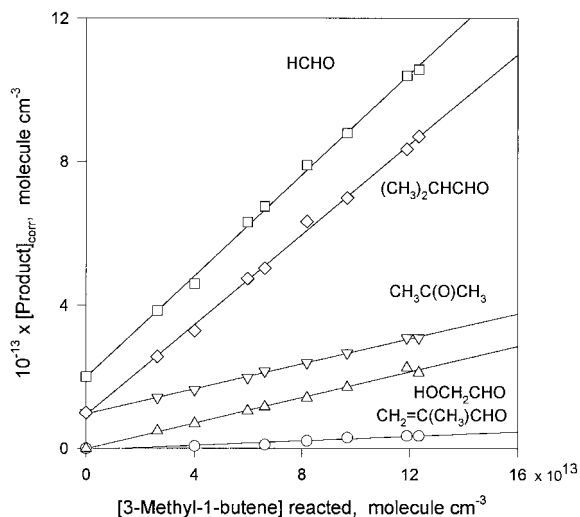


Figure 2 Plots of the amounts of HCHO, 2-methylpropanal, acetone, glycolaldehyde, and methacrolein formed, corrected for secondary reactions (see text), against the amounts of 3-methyl-1-butene reacted with the OH radical in the presence of NO for experiments carried out in an evacuable chamber with analyses by FT-IR absorption spectroscopy. The data for acetone, 2-methylpropanal, and HCHO have been displaced vertically by 1.0×10^{13} , 1.0×10^{13} , and 2.0×10^{13} molecule cm^{-3} , respectively, for clarity.

acrolein in the Teflon chamber experiments with GC-FID analyses. All of the plots shown in Figure 2 and those for 2-methylpropanal and methacrolein in Figure 3 are good straight lines, and the formation yields obtained from least-squares analyses of the data are given in Table I. Also included in Table I are the upper limits to the formation yields of methyl vinyl ketone and 3-methyl-2-butenal derived from the GC-FID analyses.

The formation yield of HCHO given in Table I is rigorously an upper limit because of formation of HCHO from acetaldehyde produced by the photolysis of ethyl nitrite. However, as discussed by Atkinson et al. [16], formation of HCHO from secondary reactions of acetaldehyde in irradiated $\text{C}_2\text{H}_5\text{ONO}-\text{NO}-3$ -methyl-1-butene-air mixtures is expected to lead to an HCHO formation yield of ≤ 0.04 , and, hence, the HCHO formation yield in Table I is almost totally that formed from the OH radical reaction with 3-methyl-1-butene. Although acetone is expected to be formed from the secondary reaction of 2-methylpropanal, there is no evidence for any departure from linearity in the plot shown in Figure 2. Furthermore, the acetone formation yield in the experiments with FT-IR analyses is identical, within the experimental uncertainties, to the yield of glycolaldehyde, the expected coproduct

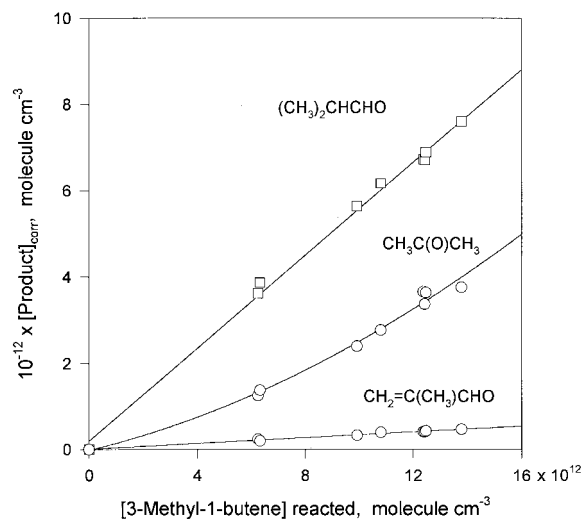


Figure 3 Plots of the amounts of 2-methylpropanal, acetone, and methacrolein formed, corrected for secondary reactions (see text), against the amounts of 3-methyl-1-butene reacted with the OH radical in the presence of NO for experiments carried out in a Teflon chamber with analyses by GC-FID. The curve shown through the acetone data points is for illustrative purposes only.

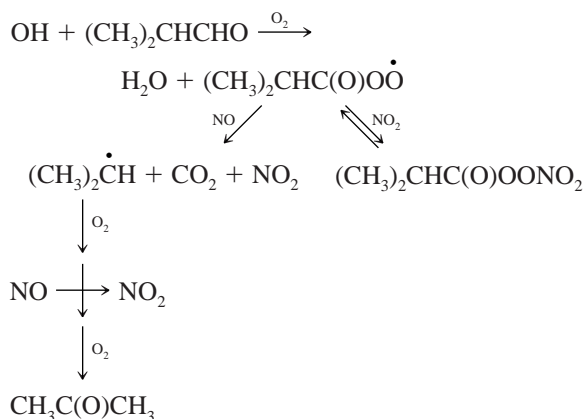
Table I Products and their Formation Yields Observed from the Reaction of the OH Radical with 3-Methyl-1-Butene in the Presence of NO at 298 ± 2 K and 740 Torr Total Pressure of Air

Product	Formation Yield	
	GC-FID analyses ^a	FT-IR analyses ^b
2-methylpropanal	0.54 ± 0.05	0.63 ± 0.05
formaldehyde		0.70 ± 0.06
acetone		0.17 ± 0.02
glycolaldehyde		0.18 ± 0.03
methacrolein	0.034 ± 0.004	0.031 ± 0.011
methyl vinyl ketone	<0.01	
3-methyl-2-butenal	<0.01	
organic nitrates ^c		ca. 0.15

^a Indicated errors are two least-squares standard deviations combined with estimated overall uncertainties in the GC-FID response factors for 3-methyl-1-butene and the products of $\pm 5\%$ each.

^b Indicated errors are two least-squares standard deviations combined with estimated overall uncertainties of $\pm 5\%$ each in the calibration and subtractive analysis of 3-methyl-1-butene, 2-methylpropanal, formaldehyde, and acetone, with corresponding uncertainties of $\pm 10\%$ and $\pm 25\%$ for glycolaldehyde and methacrolein, respectively.

^c Based on the API-MS analyses (see text), the organic nitrates are probably the β -hydroxynitrates $(\text{CH}_3)_2\text{CHCH}(\text{ONO}_2)\text{CH}_2\text{OH}$ and/or $(\text{CH}_3)_2\text{CHCH}(\text{OH})\text{CH}_2\text{ONO}_2$ formed from the reactions of the corresponding β -hydroxyalkyl peroxy radicals with NO.



Reaction Scheme IV

from decomposition of the $(\text{CH}_3)_2\text{CHCH}(\dot{\text{O}})\text{CH}_2\text{OH}$ radical (Reaction Scheme I).

The absence of an increase in the acetone yield with reaction time in the evacuable chamber experiments with FT-IR analyses can be explained if the peroxyacyl nitrate absorption bands depicted in Figure 1 are indeed those of $(\text{CH}_3)_2\text{CHC}(\text{O})\text{OONO}_2$, with the loss of 2-methylpropanal by reaction with the OH radical proceeding mainly by abstraction of the aldehydic hydrogen atom followed by steps leading to the formation of $(\text{CH}_3)_2\text{CHC}(\text{O})\text{OONO}_2$ in high yield (Reaction Scheme IV). From the amount of 2-methylpropanal present in the spectrum of Figure 1(B) and the corresponding multiplicative correction factor of 1.13, a loss of 8.9×10^{12} molecule cm^{-3} of 2-methylpropanal by secondary reaction with the OH radical can be estimated. Assuming that the integrated absorption coefficient determined for the 1741 cm^{-1} band of $\text{CH}_3\text{C}(\text{O})\text{OONO}_2$ [35] applies to the analogous 1738 cm^{-1} band of $(\text{CH}_3)_2\text{CHC}(\text{O})\text{OONO}_2$, then the latter's concentration is estimated from Figure 1(C) (after subtraction of contributions from glycolaldehyde and methacrolein) as 7.1×10^{12} molecule cm^{-3} , accounting for ca. 80% (and possibly all) of the 2-methylpropanal consumed by reaction with the OH radical.

As shown in Figure 3, the acetone yield in the experiments with GC-FID analyses clearly increases with increasing amount of 3-methyl-1-butene reacted, suggesting secondary formation from 2-methylpropanal. These experiments resulted in significantly higher conversions of 3-methyl-1-butene than was the case in the experiments with FT-IR analyses (up to 62% vs. up to 25% conversion, respectively), but employed higher initial NO/3-methyl-1-butene concentration ratios such that the final NO/NO₂ concentration ratios were ≥ 1 . Reaction of 2-methylpropanal with

the OH radical would therefore be expected to lead to the formation of acetone, at least in part [4] (Reaction Scheme IV). At the lowest extents of reaction in the experiments with GC-FID analyses, the acetone yield approached that observed in the experiments with FT-IR analyses. We therefore conclude that the acetone formation yield obtained from the experiments with FT-IR analyses conducted at low conversions of 3-methyl-1-butene, and under conditions such that $(\text{CH}_3)_2\text{CHC}(\text{O})\text{OONO}_2$ was the major product formed from the secondary reaction of 2-methylpropanal, reflects the formation of "first-generation" acetone, and this yield is given in Table I.

The yield of RONO_2 was estimated from the ca. 1280 cm^{-1} absorption band based on an average of the integrated absorption coefficients previously measured for other organic nitrates [12]. Because a peroxyacyl nitrate (assumed to be $(\text{CH}_3)_2\text{CHC}(\text{O})\text{OONO}_2$; see above) also increasingly contributed to the intensity of this band with increasing irradiation time, RONO_2 concentrations were derived from the early portions of the experiments when the spectra did not show measurable absorptions from the peroxyacyl nitrate species. Both experiments gave RONO_2 formation yields of ca. 0.15 during the early stages of irradiation, and this value is reported in Table I.

Teflon Chamber with Analyses by API-MS

API-MS spectra of irradiated $\text{CH}_3\text{ONO-NO-3-methyl-1-butene}$ -air mixtures showed the presence of ion peaks at 59, 73, 117, 131, 145, 159, 208, and 222 u. API-MS/MS "daughter ion" and "parent ion" spectra were obtained for these and other ion peaks observed in the API-MS analyses. Product ion peaks were identified based on the observation of homo- or heterodimer ions (for example, $[(M_{P1})_2 + \text{H}]^+$ and $[M_{P1} + M_{P2} + \text{H}]^+$, respectively, where P1 and P2 are products) in the API-MS/MS "parent ion" spectra, and consistency of the API-MS/MS "daughter ion" spectrum of a homo- or hetero-dimer ion with the "parent ion" spectra of the various $[M_p + \text{H}]^+$ ion peaks. The API-MS/MS spectra obtained indicated the presence of products of molecular weight 58 (attributed to acetone), 72 (attributed to 2-methylpropanal), 100, and 149. As an example of the spectra obtained, Figure 4 shows the API-MS/MS "parent ion" spectrum of the 59 u ion peak, with the dimer ions being labeled. Based on the product identifications, the ion peaks observed in the API-MS spectra at 59, 73, 117, 131, 145, 159, 208, and 222 u are then $[\text{acetone} + \text{H}]^+$, $[\text{2-methylpropanal} + \text{H}]^+$, $[\text{acetone} + \text{acetone} + \text{H}]^+$, $[\text{acetone} + \text{2-methylpropanal} + \text{H}]^+$, $[\text{2-methyl-}$

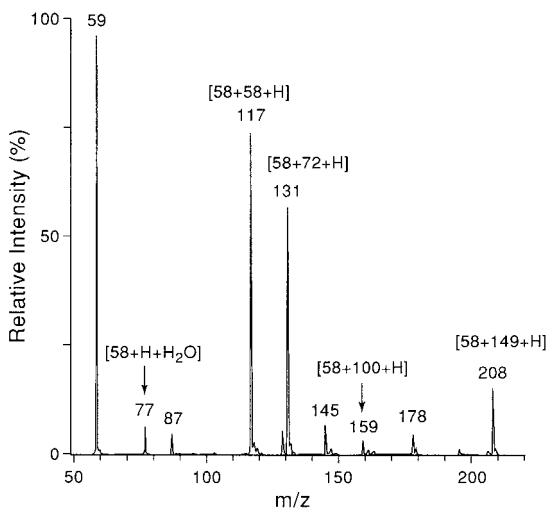


Figure 4 API-MS/MS CAD "parent ion" spectrum of the 59 u ion peak observed in the API-MS spectrum of an irradiated $\text{CH}_3\text{ONO}-\text{NO}-3\text{-methyl-1-butene}$ -air mixture. The ion peaks at 145 and 178 u are attributed to fragment ions of the 208 u ion peak (the former being a loss of HNO_3).

propanal + 2-methylpropanal + H^+ , [acetone + 100 + H^+], [acetone + 149 + H^+], and [2-methylpropanal + 149 + H^+], respectively.

The API-MS/MS "daughter ion" spectrum of the weak 150 u ion peak showed fragment ions at 132 u ($-\text{H}_2\text{O}$), 87 u ($-\text{HNO}_3$), and 46 u ($[\text{NO}_2]^+$) (Fig. 5), suggesting that the molecular weight 149 product was

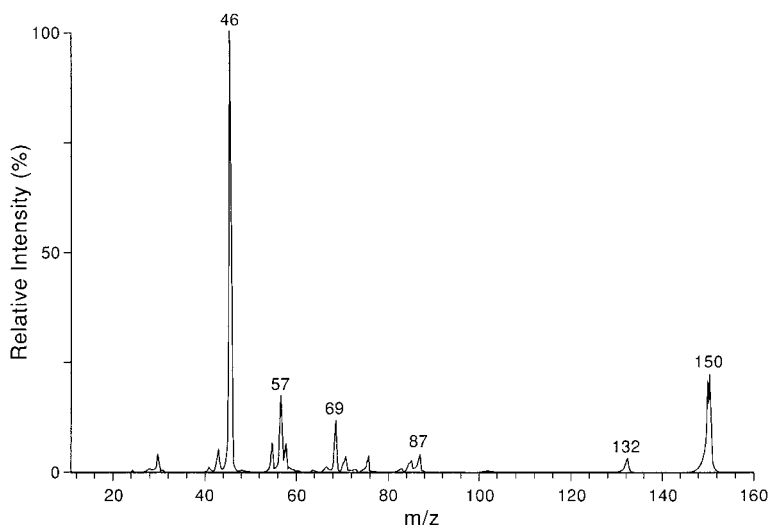


Figure 5 API-MS/MS CAD "daughter ion" spectrum of the 150 u weak ion peak observed in the API-MS spectrum of an irradiated $\text{CH}_3\text{ONO}-\text{NO}-3\text{-methyl-1-butene}$ -air mixture. The fragment ion peaks at 132 and 87 u are attributed to losses of H_2O and HNO_3 , respectively, and the 46 u ion peak is attributed to $[\text{NO}_2]^+$.

the hydroxynitrate $(\text{CH}_3)_2\text{CHCH}(\text{OH})\text{CH}_2\text{ONO}_2$ and/or $(\text{CH}_3)_2\text{CHCH}(\text{ONO}_2)\text{CH}_2\text{OH}$ formed in Reaction (6a) and its analog. The API-MS/MS "daughter ion" spectrum of the weak 101 u ion peak present in the API-MS spectrum showed fragment ions at 83, 73, 71, 59 (weak), 55, 43, 31, and 29 u and, apart from the relative intensities of the 83, 73, and 71 u peaks, was similar to the API-MS/MS spectrum of the 101 u ion peak observed in the OH radical-initiated reaction of isoprene [17]. This molecular weight 100 product may be $\text{HOCH}_2\text{C}(\text{CH}_3)=\text{CHCHO}$ (see Reaction Scheme III).

DISCUSSION

The formation yields of 2-methylpropanal measured from the GC-FID and FT-IR analyses (0.54 ± 0.05 and 0.63 ± 0.05 , respectively) differ by ca. 15%, but are in agreement within the combined overall uncertainties. The reason for this difference is not known but could be due in part to uncertainties in the rate constant ratio $k(\text{OH} + 2\text{-methylpropanal})/k(\text{OH} + 3\text{-methyl-1-butene})$ which is needed to calculate the correction factors to account for secondary reactions of 2-methylpropanal [a 10% increase in the rate constant ratio $k(\text{OH} + 2\text{-methylpropanal})/k(\text{OH} + 3\text{-methyl-1-butene})$ increases the maximum multiplicative correction factor for 2-methylpropanal by 4.2% for the experiments with GC-FID analyses and by 1.1% for the experiments with FT-IR analyses]. The

two yield determinations are averaged, resulting in a formation yield of 2-methylpropanal of 0.58 ± 0.08 .

Consistent with the reaction pathways shown in Reaction Schemes I–III, formation of 2-methylpropanal plus HCHO, acetone plus glycolaldehyde, and methacrolein plus HCHO account for $58 \pm 8\%$, $18 \pm 3\%$, and $3.3 \pm 0.7\%$ of the overall reaction products, with the molar HCHO yield of 0.70 ± 0.06 being in reasonable agreement with the sum of the 2-methylpropanal and methacrolein yields (0.61 ± 0.09). Together with the estimated yield of “organic nitrates” of ca. 0.15 during the initial portions of the experiments, 94% of the total reaction products and reaction pathways of the OH radical-initiated reaction of 3-methyl-1-butene in the presence of NO are accounted for. Furthermore, as shown by the estimated reaction rates [32] of the major alkoxy radicals involved in the OH radical-initiated reaction of 3-methyl-1-butene in the presence of NO, the observed products are consistent with the calculated dominant reaction pathways of these alkoxy radicals. No evidence for the formation of methyl vinyl ketone or 3-methyl-2-butenal was obtained, and conservative upper limits to the formation yields of these two potential H-atom abstraction pathway products (Reaction Scheme III) are given in Table I. The formation of organic nitrates during the early stages of the reaction is anticipated to arise from the reaction of the organic peroxy radicals [including $(\text{CH}_3)_2\text{CHCH}(\text{OO})\text{CH}_2\text{OH}$, $(\text{CH}_3)_2\text{CHCH}(\text{OH})\text{CH}_2\text{O}_2$, $(\text{CH}_3)_2\text{C}(\text{OO})\text{CH}=\text{CH}_2$, and $(\text{CH}_3)_2\text{C}=\text{CHCH}_2\text{O}_2$] with NO (Reaction (6a) and analogous reactions). The approximate organic nitrate formation yield of 0.15 is reasonably consistent with organic nitrate formation yield measurements for the OH radical-initiated reactions of C_4 – C_6 alkenes in the presence of NO [36–38], with reported organic nitrate yields of 0.037 ± 0.009 for the *cis*-2-butene reaction [37] and ca. 0.15 for the 2,3-dimethyl-2-butene reaction [36,38].

The API-MS and API-MS/MS analyses are consistent with the GC-FID and FT-IR analyses, with the major products being attributed to acetone, 2-methylpropanal and the β -hydroxynitrates $(\text{CH}_3)_2\text{CHCH}(\text{ONO}_2)\text{CH}_2\text{OH}$ and/or $(\text{CH}_3)_2\text{CHCH}(\text{OH})\text{CH}_2\text{ONO}_2$. The API-MS analyses also suggest the presence of a product (or products) of molecular weight 100, possibly $\text{HOCH}_2\text{C}(\text{CH}_3)=\text{CHCHO}$ and/or $\text{CH}_2=\text{C}(\text{CH}_3)\text{C}(\text{O})\text{CH}_2\text{OH}$ formed subsequent to the H-atom abstraction pathway (Reaction Scheme III).

Therefore, our data show that at room temperature and atmospheric pressure, OH radical addition dominates for 3-methyl-1-butene, with H-atom abstraction accounting for a minimum of 3.3% (based on the formation yield of methacrolein). The OH radical addi-

tion pathway accounts for $91 \pm 12\%$ of the overall OH radical reaction with 3-methyl-1-butene. Taking into account the possible formation of $\text{HOCH}_2\text{C}(\text{CH}_3)=\text{CHCHO}$ [or possibly $\text{CH}_2=\text{C}(\text{CH}_3)\text{C}(\text{O})\text{CH}_2\text{OH}$; see Reaction Scheme III] as suggested by our API-MS data and noting our upper limits to the formation of methyl vinyl ketone and 3-methyl-2-butenal of $< 1\%$ each, a reasonable estimate of the H-atom abstraction pathway in the reaction of the OH radical with 3-methyl-1-butene is 5–10%. Combined with previous literature data [4,8,9,11], this suggests that H-atom abstraction from the allylic C—H bonds of alkenes during the OH radical reactions is of minor importance, accounting for only a few percent of the overall reactions under tropospheric conditions.

The authors gratefully thank the U.S. Environmental Protection Agency, Office of Research and Development (Assistance Agreement R-825252-01-0) for supporting this research, and thank the National Science Foundation (Grant No. ATM-9015361) and the University of California, Riverside, for funds for the purchase of the SCIEX API III MS/MS instrument. While this research has been supported by the U.S. Environmental Protection Agency, it has not been subjected to Agency review and, therefore, does not necessarily reflect the views of the Agency, and no official endorsement should be inferred.

BIBLIOGRAPHY

1. R. L. Seila, W. A. Lonneman, and S. A. Meeks, *Determination of C_2 to C_{12} Ambient Air Hydrocarbons in 39 U.S. Cities, from 1984 through 1986*, U.S. Environmental Protection Agency Report EPA/600/3-89/058, Atmospheric Research and Exposure Assessment Laboratory, Research Triangle Park, North Carolina, September 1989.
2. F. W. Lurmann and H. H. Main, *Analysis of the Ambient VOC Data Collected in the Southern California Air Quality Study*, Final Report to California Air Resources Board Contract No. A832-130, Sacramento, CA, February 1992.
3. W. L. Chameides, F. Fehsenfeld, M. O. Rodgers, C. Cardelino, J. Martinez, D. Parrish, W. Lonneman, D. R. Lawson, R. A. Rasmussen, P. Zimmerman, J. Greenberg, P. Middleton, and T. Wang, *J. Geophys. Res.*, **97**, 6037 (1992).
4. R. Atkinson, *J. Phys. Chem. Ref. Data*, **Monograph 2**, 1 (1994).
5. R. Atkinson, *J. Phys. Chem. Ref. Data*, **26**, 215 (1997).
6. N. J. Blake, S. A. Penkett, K. C. Clemitshaw, P. Anwyl, P. Lightman, A. R. W. Marsh, and G. Butcher, *J. Geophys. Res.*, **98**, 2851 (1993).
7. R. Atkinson, *Gas Phase Tropospheric Chemistry of Organic Compounds*, **In Volatile Organic Compounds in**

- the Atmosphere, Issues in Environmental Science and Technology*, **4**, Eds. R. E. Hester and R. M. Harrison, The Royal Society of Chemistry, Cambridge, UK, 1995, pp. 65–89.
8. R. Atkinson, *J. Phys. Chem. Ref. Data*, **Monograph 1**, 1 (1989).
 9. H. Niki, P. D. Maker, C. M. Savage, and L. P. Breitenbach, *J. Phys. Chem.*, **82**, 135 (1978).
 10. H. Niki, P. D. Maker, C. M. Savage, and L. P. Breitenbach, *Chem. Phys. Lett.*, **80**, 499 (1981).
 11. R. Atkinson, E. C. Tuazon, and W. P. L. Carter, *Int. J. Chem. Kinet.*, **17**, 725 (1985).
 12. E. C. Tuazon and R. Atkinson, *Int. J. Chem. Kinet.*, **22**, 1221 (1990).
 13. S. E. Paulson, R. C. Flagan, and J. H. Seinfeld, *Int. J. Chem. Kinet.*, **24**, 79 (1992).
 14. S. E. Paulson and J. H. Seinfeld, *Environ. Sci. Technol.*, **26**, 1165 (1992).
 15. A. Miyoshi, S. Hatakeyama, and N. Washida, *J. Geophys. Res.*, **99**, 18779 (1994).
 16. R. Atkinson, E. C. Tuazon, and S. M. Aschmann, *Environ. Sci. Technol.* **29**, 1674 (1995).
 17. E. S. C. Kwok, R. Atkinson, and J. Arey, *Environ. Sci. Technol.* **29**, 2467 (1995).
 18. E. S. C. Kwok, R. Atkinson, and J. Arey, *Environ. Sci. Technol.* **30**, 1048 (1996).
 19. G. P. Smith, *Int. J. Chem. Kinet.*, **19**, 269 (1987).
 20. K. Hoyer mann and R. Sievert, *Ber. Bunsenges. Phys. Chem.*, **83**, 933 (1979).
 21. K. Hoyer mann and R. Sievert, *Ber. Bunsenges. Phys. Chem.*, **87**, 1027 (1983).
 22. D. F. McMillen and D. M. Golden, *Ann. Rev. Phys. Chem.*, **33**, 493 (1982).
 23. J. A. Kerr, *Strengths of Chemical Bonds*, in *Handbook of Chemistry and Physics*, 74th Ed., Ed. D. R. Lide, CRC Press, Boca Raton, FL, 1993–94, pp. 9-123 to 9-145.
 24. R. Atkinson, W. P. L. Carter, A. M. Winer, and J. N. Pitts, Jr., *J. Air Pollut. Control Assoc.*, **31**, 1090 (1981).
 25. R. Atkinson and S. M. Aschmann, *Environ. Sci. Technol.*, **27**, 1357 (1993).
 26. S. M. Aschmann and R. Atkinson, *Environ. Sci. Technol.*, **28**, 1539 (1994).
 27. E. C. Tuazon and R. Atkinson, *Int. J. Chem. Kinet.*, **21**, 1141 (1989).
 28. R. Atkinson, E. S. C. Kwok, J. Arey, and S. M. Aschmann, *Faraday Discuss. Chem. Soc.*, **100**, 23 (1995).
 29. E. S. C. Kwok, J. Arey, and R. Atkinson, *J. Phys. Chem.* **100**, 214 (1996).
 30. E. S. C. Kwok and J. Arey, to be submitted for publication (1998).
 31. W. D. Taylor, T. D. Allston, M. J. Moscato, G. B. Fazekas, R. Kozlowski, and G. A. Takacs, *Int. J. Chem. Kinet.*, **12**, 231 (1980).
 32. R. Atkinson, *Int. J. Chem. Kinet.*, **29**, 99 (1997).
 33. E. S. C. Kwok and R. Atkinson, *Atmos. Environ.*, **29**, 1685 (1995).
 34. R. Atkinson, S. M. Aschmann, W. P. L. Carter, A. M. Winer, and J. N. Pitts, Jr., *J. Phys. Chem.*, **86**, 4563 (1982).
 35. N. Tsalkani and G. Toupance, *Atmos. Environ.*, **23**, 1849 (1989).
 36. H. Niki, P. D. Maker, C. M. Savage, L. P. Breitenbach, and M. D. Hurley, *J. Phys. Chem.*, **91**, 941 (1987).
 37. K. Muthuramu, P. B. Shepson, and J. M. O'Brien, *Environ. Sci. Technol.*, **27**, 1117 (1993).
 38. E. C. Tuazon, S. M. Aschmann, J. Arey, and R. Atkinson, *Environ. Sci. Technol.*, in press (1998).